coatings

MDPI

Article

Rf-Sputtered Teflon®-Modified Superhydrophobic Nanostructured Titanium Dioxide Coating on Aluminum Alloy for Icephobic Applications

Saleema Noormohammed * and Dilip Kumar Sarkar

Department of Applied Science, University of Québec at Chicoutimi, Aluminum Research Center – REGAL, Saguenay, QC G7H 2B1, Canada; dsarkar@uqac.ca

* Correspondence: snoormoh@uqac.ca

Abstract: Icing on surfaces such as cables or high-voltage insulators may often lead to severe safety issues such as power outages in cold winter conditions. Conventional methods used to tackle such icing problems include mechanical deicing, where the ice is scraped or broken, and chemical deicing, where deicers such as ethylene glycol are used. However, the best approach to addressing these issues is to prevent ice formation in the first place. Research in the past few decades have shown hydrophobic and superhydrophobic surfaces to be effective in reducing ice adhesion. We used the concept of water repellency to turn an aluminum surface superhydrophobic to minimize ice adhesion on these surfaces. However, to render these surfaces also applicable to insulating surfaces, we also demonstrated the adaptability of the concept on a low dielectric oxide, TiO_2, to an aluminum surface with icephobic properties. This work demonstrates the importance of the coexistence of rough nanostructures as well as low-surface-energy compositions on a surface to make it superhydrophobic and icephobic and is applicable on metals and insulating surfaces.

Keywords: superhydrophobic; icephobic; TiO_2; aluminum alloy; low surface energy; water contact angle; sol–gel coating; rf-sputtered Teflon®

Citation: Saleema, N.; Sarkar, D.K. Rf-Sputtered Teflon®-Modified Superhydrophobic Nanostructured Titanium Dioxide Coating on Aluminum Alloy for Icephobic Applications. *Coatings* **2021**, *11*, 432. https://doi.org/10.3390/coatings11040432

Received: 2 February 2021
Accepted: 5 April 2021
Published: 9 April 2021

1. Introduction

Ice adheres strongly to almost all kinds of surfaces. It is a known fact that the strong adhesion of ice to various surfaces such as aircraft parts, streets and sidewalks, automobile windshields, conducting cables, and insulator surfaces poses a major inconvenience or even a significant danger challenging public safety as well as industry operations. "The Great Ice Storm" of January 1998 deprived millions of Québec and Ontario residents of electricity for up to 30 days [1] after collapsing many power lines and more than 1000 pylons, causing more than 25 fatalities due to reasons related to power outages and leading to hundreds of millions of dollars in damage, is a classic example of an ice accumulation-related major catastrophe. There has been many more such winter classic catastrophes [1,2]. For example, the Continental commuter flight 3407 crash, which claimed 50 lives, was due to icing on the wings and cockpit windshields. The need to scrape ice that forms on automobile windshields is regarded by most drivers as a bothersome and recurring chore, and any residual ice impairs visibility and safety. At least 150 telecommunications towers have collapsed due to ice loads in the last half century. Similarly, ice accretion, together with superimposed contamination, often causes a decrease in the flashover voltage of outdoor insulators, resulting in occasional outages. It has been reported that, in North America and Northern Europe, many power utilities have suffered network disturbances caused by the effect of ice and/or snow accumulation on insulators [3]. Insulation failures due to the ice-bridging of insulators are also reported in the USA, Canada, Japan, Norway, China, and several other countries [4].

Removing the highly adhered ice from a surface is not an easy task. The adhesion strength of ice on surfaces such as steel or aluminum can vary from ≈0.03 MPa to as high as ≈2 MPa depending on the test conditions and the roughness of the surface [5]. Existing strategies to eliminate or remove ice from surfaces include chemical, mechanical, or thermal deicing; however, these methods carry several disadvantages. Deicing techniques such as the use of freezing point depressants, such as salt or chemical sprays, have been employed on highways [1]. Deicing fluids such as ethylene glycol and propylene glycol are used on aircraft wings and have been found to be effective [1]. The drawback in such deicing techniques is the need to apply and maintain a sufficient quantity of deicers, which is both time-consuming and expensive. Furthermore, the deicing fluids are toxic and environmentally unsafe. Mechanical and chemical removal of ice cause great damage to surfaces and are mostly expensive, while heating to melt the accumulated ice requires a large energy supply [6]. All these methods refer to removal of already formed strongly adhered ice build-up, but none of these techniques prevent ice from forming. Therefore, it becomes of significant importance to prevent ice from adhering to substrate surfaces or to minimize the strength of adhesion of ice to the surfaces by applying coatings with icephobic properties.

Ice is generally accreted during periods of sub-zero temperatures by the impact of supercooled droplets of water onto the surface. A more practical and economical choice in the prevention of ice formation on surfaces at sub-zero temperatures is to apply a coating that is icephobic in nature, so that ice does not adhere to the surfaces. Studies have suggested that this may be achievable if the surface is made superhydrophobic, to which water does not stick but rather rolls off the surface [7–12]. Superhydrophobicity is observed on certain natural tissues such as lotus leaves and butterfly wings [13,14]. The so-called "Lotus effect" is due to the presence of a rough micro-nanostructure covered with waxy materials that are poor for wetting, resulting in a water contact angle greater than 150° [13]. The rough micro-nanostructure allows the entrapment of air beneath the water drop in the pores (troughs) of the rough structure and the waxy coating, which has a low surface energy, and helps to reduce the interaction of the surface with water. Learning from nature, a superhydrophobic surface can be obtained by creating optimal surface roughness followed by passivation with a low-surface-energy coating leading to a very low area of contact between the solid surface and the liquid, causing a water drop to roll off the surface. As the contact area of water on a superhydrophobic solid surface is negligible, such surfaces would effectively reduce the contact area of ice as well. Therefore, ice adhesion would be significantly reduced on superhydrophobic surfaces. There have been several advances in rendering aluminum and metal surfaces superhydrophobic by different methods, all of which involves combining a rough microstructure with a low-surface-energy coating either by one- or two-step processes employing diverse preparation routes [15–17]. However, ice adhesion has also been reported to vary as a function of the dielectric nature of the coating due to mirror charge screening effects, as reported previously [1,18]. A dielectric material's surface is therefore expected to play an important role in the possible elimination of one of the strongest interaction forces: the electrostatic forces of attraction at the ice–surface interface. Therefore, a combination of dielectric materials and superhydrophobicity is expected to perform well in terms of reduction in ice adhesion. Although several studies show significant improvement in water repellency and a few studies on ice adhesion improvement on aluminum surfaces, the effect of the presence of a dielectric coating on aluminum has not been explored [1].

In view of the application on both conducting and insulating surfaces, we created aluminum alloy surfaces (metal) as well as titanium dioxide (ceramic) coatings on aluminum alloy surfaces with very high superhydrophobicity and negligible ice adhesion. Aluminum surfaces were modified with a TiO_2 coating prior to Teflon® sputtering to make the surface dielectric. Rough nanostructures created by chemical etching on aluminum surfaces with or without TiO_2 coating were modified with low-surface-energy radio frequency (rf)-sputtered Teflon® coating resulting in very high water contact angles (>160°)

and very low hysteresis (<5°). TiO_2 coatings were performed by the sol–gel technique on the nanostructured aluminum surfaces. The coexistence of rough nanostructures and low-surface-energy components is essential in this study and is key to achieving both superhydrophobic and icephobic properties.

2. Experimental

Rough nanostructures were created on ultrasonically clean AA6061 aluminum alloy surfaces by chemical etching using 40 vol% aqueous hydrochloric acid (HCl) for about three minutes. The etched coupons were rinsed under tap water to stop further reactions followed by ultra-sonication in de-ionized water to remove any debris. The cleaned etched Al alloy surfaces were then dried in an oven for several hours to remove excess water prior to coating with TiO_2 or rf-sputtered Teflon®.

A stock solution of TiO_2 sol with varied molar concentration (0.10–0.30 M) was prepared by diluting the tetrabutoxy titanium (TBOT, $C_{16}H_{36}O_4Ti$) precursor (from Sigma Aldrich, St. Louis, MO, USA) with ethanol at a 1:1 volume ratio under constant stirring at 500 rpm for 10 min at room temperature. The stock TiO_2 sol, aged for 48 h, was deposited dropwise onto an ultrasonically cleaned Si(100) surface (for thickness measurements only), spread using a spin-coater (Laurell Tech, model WS-400B-6NPP, North Wales, PA, USA) at 4000 rpm for 30 s, dried on a hotplate at 120 °C for 30 min, and annealed in air at 450 °C for 30 min. Rutherford backscattering spectrometry (RBS, IGCAR, Kalpakkam, India) was used for elemental depth profiling using 2 MeV He ions, and spectra from silicon and germanium samples were used for calibration. A GISA-3 software was used to obtain the TiO_2 coating thickness on flat aluminum surfaces. The crystal structure of these films were investigated by X-ray diffraction (XRD, Siemens, IGCAR, Kalpakkam, India).

Sol–gel TiO_2 coating with select thicknesses, selected based on RBS measurements on Si(100) surfaces, was used for coating the nanostructured aluminum alloy surfaces to obtain an oxide coating. The nanostructured Al alloy surfaces as well as the TiO_2-coated nanostructured Al alloy surfaces were both modified by applying rf-sputtered Teflon® coating on these surface to make them superhydrophobic. Teflon® was sputtered onto these surfaces using an Ar plasma in an inductively coupled plasma reactor (Plasmionique Inc., Varennes, QC, Canada) by applying a power of 50 W. The distance between the Teflon® target and the substrate was 30 cm. The sputtering process was carried out for ≈20 min at an Ar pressure of 20 mTorr in the chamber during process. The base pressure was 2×10^{-6} Torr.

Field emission scanning electron microscopy (FEGSEM, LEO 1525) and X-ray photoelectron spectroscopy (XPS, ESCALAB 220iXL, INRS-ÉMT, Varennes, QC, Canada) were used for surface morphological and chemical compositional analyses of all surfaces studied. A contact angle goniometer (Krüss GmbH, Hamburg, Germany) was used to investigate the wettability of the prepared surfaces. Five microliter volume droplets were used to measure the static, advancing, and receding contact angles. The static contact angle data were acquired by fitting the symmetric water drops using the Laplace–Young equation and the advancing and receding contact angles were determined from the asymmetric, water drops using the tangent-2 method [19].

For icephobicity tests, the samples were performed by exposing the sample surfaces to a freezing drizzle of supercooled water droplets at −10 °C in a wind tunnel at a fixed wind speed of 10 m/s in order to simulate atmospheric icing conditions in natural outdoor situations. The identification details of the samples tested for icephobicity as well as superhydrophobicity are provided in Table 1. The samples mounted on untreated supports were placed vertically in a wind tunnel perpendicular to the direction of flow of the freezing drizzle. Following the accumulation of ice on the sample surfaces, the adhesion strength of ice was determined using a centrifugal ice adhesion test apparatus (CAT, CIGELE, UQAC, Canada) [20]. In this method, an aluminum beam (32 mm wide and 30 cm long) with the test sample (32 mm × 50 mm) and accumulated ice attached to one end and a counter weight attached to the other end to balance the beam was fixed in the centrifuge

test chamber maintained at −10 °C. The beam was then rotated at increasing speeds, resulting in a controlled ramp up of the centrifugal force. When this force reached the adhesion force of ice, the ice detached from the sample surface. The exact rotation speed at the time of ice detachment was determined by an integrated computer software. The adhesion force F was then determined using the formula $F = mr\omega^2$, where m is the mass of ice, r is the radius of the beam, and ω is the rotation speed. The shear adhesion strength ($\tau = F/A$) of ice was then determined from the apparent area A of the sample surface that was in contact with ice.

Table 1. Information on samples tested for superhydrophobicity and icephobicity.

Sample Name	Description
Al	Ultrasonically clean AA6061 bare Al alloys
Tef/Al	Rf-sputtered Teflon® coated Al
ns-Al	HCl etched nanostructured Al
Tef/ns-Al	Rf-sputtered Teflon® coated ns-Al
TiO_2/Al	Sol-gel TiO_2 coated Al
Tef/TiO_2/Al	Rf-sputtered Teflon® coated TiO_2/Al
TiO_2/ns-Al	Sol-gel TiO_2 coated ns-Al
Tef/TiO_2/ns-Al	Rf-sputtered Teflon® coated TiO_2/ns-Al

3. Results and Discussion

Nanostructured patterns were created on aluminum alloy surfaces (ns-Al) by reacting the clean aluminum alloy substrates in dilute aqueous hydrochloric acid solution. During this reaction of aluminum with HCl, the aluminum was etched, resulting in the creation of a certain rough nanopattern on its surface as revealed by the FESEM image shown in Figure 1. The inset of Figure 1 shows the image of an ultrasonically cleaned aluminum surface prior to HCl etching, revealing a microscopically flat surface nature.

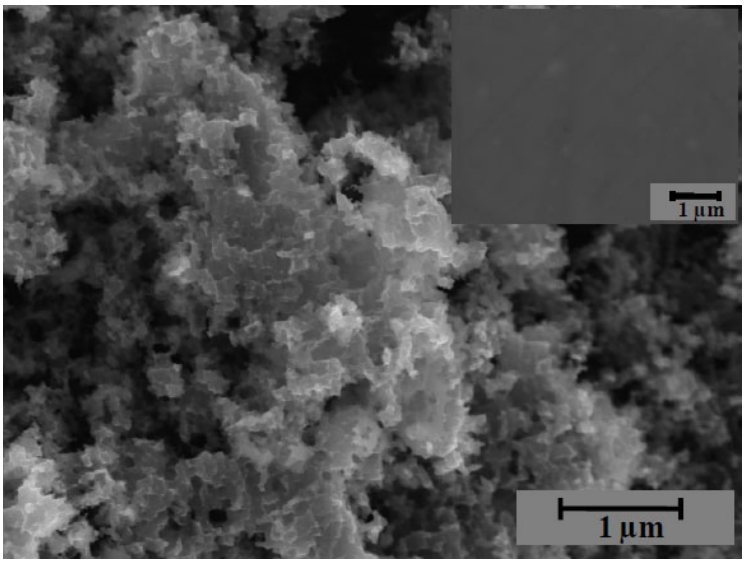

Figure 1. FESEM image of a HCl-etched nanostructured aluminum alloy surface; the inset shows the image of a clean aluminum alloy surface before etching.

The rough nanostructure obtained on the aluminum surface following etching as evident from the FESEM images when modified with a low-surface-energy coating may render the surface superhydrophobic with very low affinity to water, preventing ice from adhering to it [7–9,21].

Given the importance of the nanostructured pattern in obtaining superhydrophobic properties and with the aim of obtaining superhydrophobic, and therefore icephobic, TiO_2-coated aluminum surfaces, the ns-Al surfaces were further coated with TiO_2 by the sol–gel technique. However, in order to obtain a stable dielectric coating of TiO_2, the thickness of the TiO_2 coating was optimized using RBS spectroscopy for various molar concentrations of the TiO_2 sol prepared using a TBOT precursor. The molar concentration was varied between 0.10 and 0.30 M. In order to obtain a microscopically flat and smooth surface for precise RBS depth profiling, clean Si(100) substrates were used for coating TiO_2 with varied molar concentrations. Figure 2 shows the RBS spectra of these coatings and Table 2 shows the thickness information obtained using GISA 3 software. The thickness of the films systematically varied between 35 and 125 nm and is found to increase with increasing molar concentration of the sol.

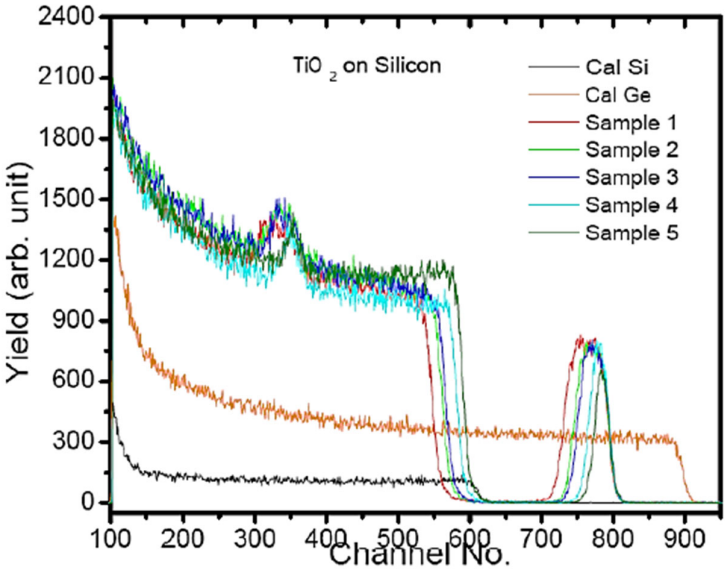

Figure 2. Rutherford backscattering spectrometry (RBS) spectra of TiO_2 films deposited on flat Si(100) surfaces using varied molar concentrations (0.10–0.30 M) of TiO_2 sol for thickness optimization.

Table 2. TiO_2 thickness derived from RBS analysis using GISA-3 software.

Sample #	Molar Conc. Of TiO_2 Sol (M)	Thickness (nm)	Composition (At%)	
			Ti	O
1	0.30	125	33.3	66.7
2	0.25	100	33.3	66.7
3	0.20	85	33.3	66.7
4	0.15	55	33.3	66.7
5	0.10	35	33.3	66.7

The XRD measurements of the different films confirmed that the sol–gel TiO_2 thin films are composed of the anatase phase [22,23]. Figure 3 shows the XRD spectra of the TiO_2 films of varying thicknesses within 2θ values between 20° and 55°. The intensities of the A(101), A(004), and A(200) peaks clearly increase with increasing molar concentrations of the sol complementing the RBS measurements.

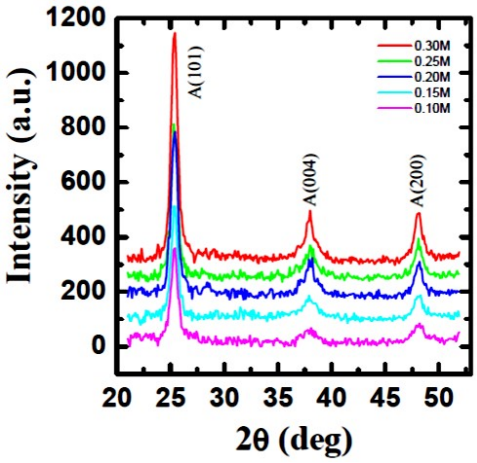

Figure 3. XRD pattern of sol–gel derived TiO_2 films of varying thicknesses coated on Si (100) substrates (A = Anatase phase of TiO_2).

It has been reported previously by Sarkar et al. that stable dielectric properties were achieved on sol–gel TiO_2 thin films coated on silicon substrates surfaces with a thickness of 100 nm. They reported a dielectric constant of 80 on these films. Stable dielectric properties are of great importance for application on insulating surfaces. Due to a similar approach used in the current study for TiO_2 coating, the films providing 100 nm thicknesses achieved using 0.25 M sol concentration were used further for application on ns-Al surfaces to result in nanostructured TiO_2-coated aluminum alloy surfaces (TiO_2/ns-Al) [22,23]. The FESEM image of the TiO_2/ns-Al surface presented in Figure 4 shows that the morphology remains unaltered following TiO_2 coating and retains the features of the ns-Al surface. The TiO_2/ns-Al surfaces were further modified with a rf-sputtered Teflon® coating to lower their surface energy and to enhance their properties toward superhydrophobicity. Similar to TiO_2/ns-Al surfaces, the morphological features were found to be retained following deposition of the Teflon® TiO_2/ns-Al surfaces as revealed by FESEM analysis (Figure not shown). Rf-sputtered Teflon® was also coated on ns-Al surfaces for a comparative analysis of superhydrophobicity and icephobicity; these surfaces also showed no alteration in their morphological features.

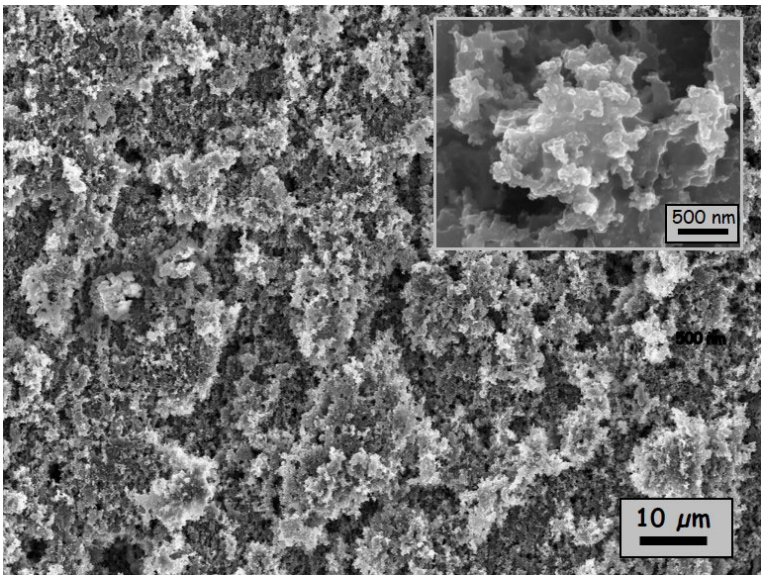

Figure 4. FESEM image of TiO_2/ns-Al; the inset shows a high-magnification image.

Furthermore, the presence of TiO_2 and rf-sputtered Teflon® on the ns-Al surfaces was confirmed from the XPS spectra. Figure 5 shows the survey spectrum of TiO_2/ns-Al revealing strong signals of Ti 2p and O 1s and a strong Ti LMM Auger peak. The Ti $2p_{3/2}$ and Ti $2p_{1/2}$ peak binding energies were 458.85 eV and 464.53 eV, respectively, and the O 1s corresponding to TiO_2 was found at 530.1 eV.

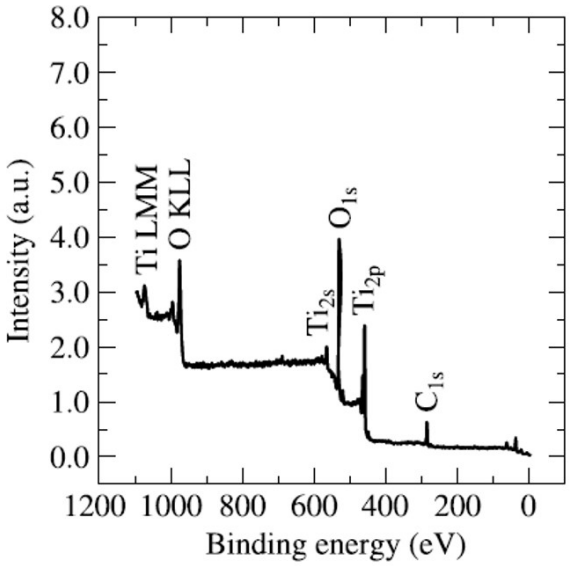

Figure 5. XPS survey spectrum of the sol–gel TiO_2 coating (TiO_2/ns-Al).

Figures 6 and 7 show, respectively, the survey spectrum and the high-resolution XPS high resolution core-level C 1s spectrum of an rf-sputtered Teflon® coating. The survey spectrum shows strong peaks of C and F, confirming the presence of a coating of Teflon®.

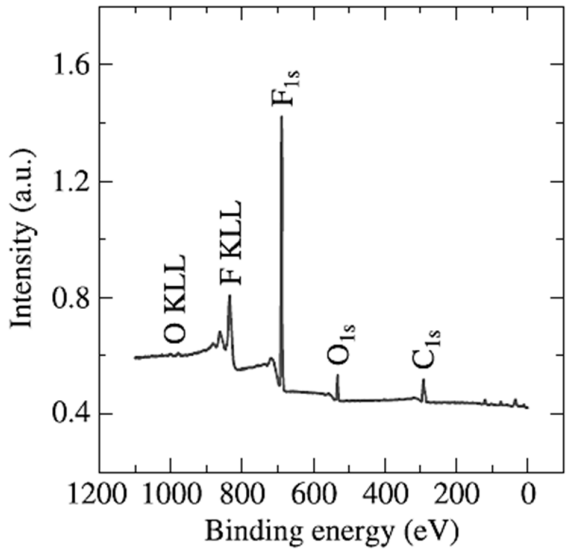

Figure 6. XPS survey spectrum of an rf-sputtered Teflon® coating on ns-Al (Tef/ns-Al).

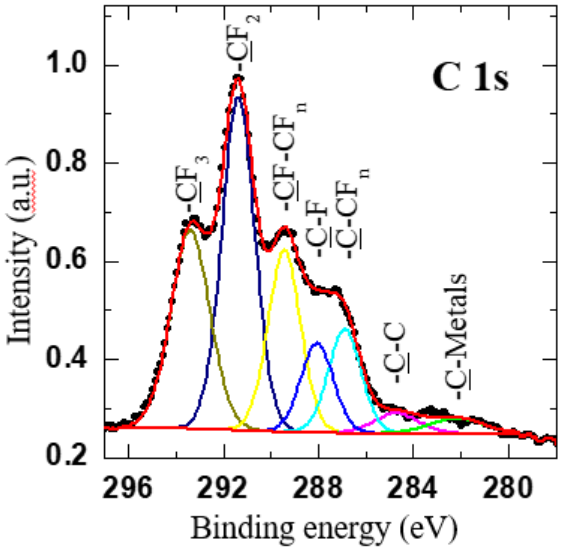

Figure 7. XPS high resolution spectra of C 1s representing an rf-sputtered Teflon® coating on ns-Al (Tef/ns-Al).

The C 1s core level spectrum (Figure 7) was resolved into seven components, namely, –CF_3 (293.50 eV), –CF_2 (291.43 eV), –CF–CF_n (289 35 eV), –C–F (287 84 eV), –C–CF_n (286 92 eV), –C–C (285 eV), and –C–Metals (283.20 eV). The relative proportions of all these components reveal higher concentrations of the low-energy surface energy groups–CF_3 (22.35%) and–CF_2 (37.66%) in contrast to other previous reports, which hardly show any CF_3 peak. This high concentration of the CF_3 peak indicates that more of these components are oriented outward from the surface [15,24].

The combination of the presence of rough nanostructures of ns-Al as well as TiO_2/ns-Al as revealed by FESEM images and that of low-surface-energy CF peaks present the potential of these surfaces to be highly superhydrophobic and, therefore, icephobic. In order to investigate these properties on these surfaces and with the view of comparative analysis to extract the advantages of improved morphology and chemistry, a combination of samples listed in Table 1 were further subjected to water contact angle studies and ice adhesion tests.

Table 3 summarizes the water contact angle data and their respective ice adhesion tests obtained from the CAT method. The water drops spread completely on ns-Al surfaces, showing 100% hydrophilic behaviour, while the clean bare aluminum surface showed a CA value of ≈74°, still in the hydrophilic zone below 90° with high contact angle hysteresis impossible to be measured. The complete spread of water drops was also witnessed on TiO_2/ns-Al, making it non-applicable (N/A) to measure CAH values. Whether non-textured or nanostructured, once the surfaces were coated with rf-sputtered Teflon®, the contact angle values increased. The highest contact angles (>160°) and lowest CAHs (<5°) were obtained on the nanostructured sample surfaces coated with rf-sputtered Teflon® irrespective of the presence of the underlying TiO_2 layer. The water drops simply rolled off these surfaces with the slightest tilt, supporting the low CAH values, which is the difference between advancing and receding contact angles (CAs) and indicates negligible contact of water with the surface. This kind of behaviour of rolling drops may be attributed to the entrapment of air in the troughs of the nanostructure as seen in the FESEM images, which reduces the area of contact with the droplet as well as to the presence of low-surface-energy C–F components as confirmed by XPS analysis. The contact fraction of the Tef/ns-Al and Tef/TiO_2/ns-Al surfaces as calculated from Cassie–Baxter equation [25] using the contact angle data obtained was found to be as low as ≈0.1 and ≈0.09, respectively, indicating negligible contact area of water with these surfaces. The

wettability behaviour, therefore, shows no difference irrespective of whether a TiO_2 layer was present beneath the rf-sputtered Teflon® coating. These observations demonstrate the importance of the coexistence of surface roughness and a low-surface-energy coating in obtaining superhydrophobic properties as emphasized in previous studies [7–10,21].

Table 3. Ice adhesion strength, water contact angle, and contact angle hysteresis data.

Samples	CA (Degree)	CA Hysteresis (Degree)	Adhesion Strength (kPa)
Al	74 ± 3	N/A (high)	420 ± 27
Tef/Al	116 ±2.5	N/A (high)	188 ± 12
ns-Al	100% spread	N/A	466 ± 122
Tef/ns-Al	165 ± 2	≤5	133 ± 13
TiO_2/Al	36 ± 2	N/A	460 ± 75
Tef/TiO_2/Al	121 ± 3	N/A (high)	138 ± 18
TiO_2/ns-Al	100% spread	N/A	480 ± 60
Tef/TiO_2/ns-Al	163 ± 3	≤5	122 ± 30

All samples listed in Table 1 underwent ice adhesion tests. An attempt was made to initiate the formation of ice and to continue its accumulation by exposing the samples surfaces to simulated freezing rain in a wind tunnel. It was observed that the ice formed and continued to accumulate on the samples that showed high wettability characteristics (hydrophilic) as soon as the supercooled water droplets came into contact. The superhydrophobic surfaces, on the other hand, showed no ice formation and, therefore, no accumulation of ice from the freezing drizzle. This highly icephobic behaviour may be attributed to the combination of the rough nanostructure and the low-surface-energy C–F components present on the surface. Some improvement in the past has been reported on hydrophobic surfaces in terms of ice adhesion, however, not completely icephobic as seen in the current study [26,27]. The CAT adhesion measurements were further carried out on the ice-accumulated hydrophilic samples as well as the slightly hydrophobic samples where ice was found to accumulate, namely, rf-sputtered Teflon®-coated non-textured (flat) surfaces. Bare aluminum (Al) was tested several times with the CAT apparatus prior to testing the samples, and an adhesion strength of ≈420 kPa obtained was confirmed against the literature values [20,28,29]. The ice adhesion strength obtained on the ns-Al surface was found to be ≈466 kPa, and that on the TiO_2/ns-Al at ≈480 kPa was similar and comparable to that on bare aluminum, as summarized in Table 3. These observations show that the adhesion of ice is stronger on hydrophilic surfaces and weaker on superhydrophobic surfaces, as evident from Table 3. The weaker adhesion strength of ice on superhydrophobic surfaces shows that these surfaces repel both room temperature and supercooled water drops. Sarkar et al. [15] have previously shown that room temperature water droplets roll off superhydrophobic aluminum surfaces prepared via a similar chemical etching process followed by rf-sputtered Teflon® coating. Teflon® has a very low surface energy of ≈18 mJ/m^2 [29] and, therefore, has very low affinity towards water. It has been reported by Bain and Whitesides that the depth of interaction of water with a surface is only 0.5 nm [30]. Therefore, the superhydrophobic and icephobic behaviour of all nanostructured samples surfaces actually does not depend on what lies beneath that 0.5 nm depth from the surface downward. This fact of the limited interaction of the depth of water with the surface indicates that the mirror charge effect is actually suppressed as the dielectric coating of TiO_2 beneath the Teflon does not interact with water or ice, but it is only the Teflon® coating over the TiO_2 that interacts with water or ice. This indicates the importance of having a rough microstructure in combination with a low-surface-energy component on the microstructure to obtain reduced affinity to water or ice. The nature of a coating or material where a microstructure is created and modified to lower its surface energy is not a major player. However, the possibility of obtaining water or ice reduction with TiO_2 coating indicates promises to be used in applications where a dielectric material

or an oxide material is required. Furthermore, Teflon® itself is dielectric with a dielectric constant of ≈2, and rf-sputtered Teflon® is also known to be a robust coating due to the strong chemical interlinking of the C–F fragments formed upon sputtering, thus presenting better physical properties, unlike other weak coatings such as the formation of aluminum hydroxide on aluminum surfaces by immersion in boiling water, as reported by Jafari et al., which is known to have a weak interface between the hydroxides and the substrate surface. Such surfaces may present excellent superhydrophobic properties [31] but may not retain their properties as they are physically weak. Similarly, chemical modification using low-surface-energy fatty acids such as stearic acid [9] or silanes [21] may also suffer in mechanical strength with the substrate while their chemical bonds may be considered stable.

Furthermore, the surfaces were also subjected to water contact angle measurements and SEM/EDX analysis following ice detachment after the ice adhesion tests to understand the coating durability. The superhydrophobic properties remained unaltered as the water contact angle and contact angle hysteresis remained in the same range (CA 160 ± 3° and CAH 3 ± 2°) following ice detachment. In addition, the EDX spectra of elemental composition shown in Figure 8 confirmed that the chemical composition remained apparently unaltered following ice detachment. The SEM image confirmed that the microstructure remained intact microscopically (figure not shown to avoid repeated image types). These observations reveal that the microstructures created as well as the chemical characteristics obtained following chemical etching of Al and/or TiO_2 coating and rf-sputtered Teflon coating have not been altered following ice detachment, indicating the durability of the coating. Studies in literature have shown similar behaviours on superhydrophobic surfaces following several icing–deicing cycles. For example, Milles et al. have shown that their microstructure produced by texturing on aluminum surfaces was stable even after 10 icing–deicing cycles [32]. In this work, due to the very low (0.5 nm) interaction depth of water indicating that the contact of ice or water is with Teflon® alone irrespective of whether a coating lies beneath the Teflon® layer, we extended our ice adhesion tests to a second iteration on a rf-sputtered Teflon®-coated superhydrophobic Al surface, however, without TiO_2 coating. The adhesion strengths remained similar and unaltered by the second accumulation and detachment of ice from these surfaces. The surfaces retained their chemical composition, as confirmed by XPS analysis, as well as their superhydrophobic properties, as revealed by the contact angle measurements (figures not shown). This observation indicated that the surfaces remained robust after a second icing/deicing cycle, as supported by literature reports [32].

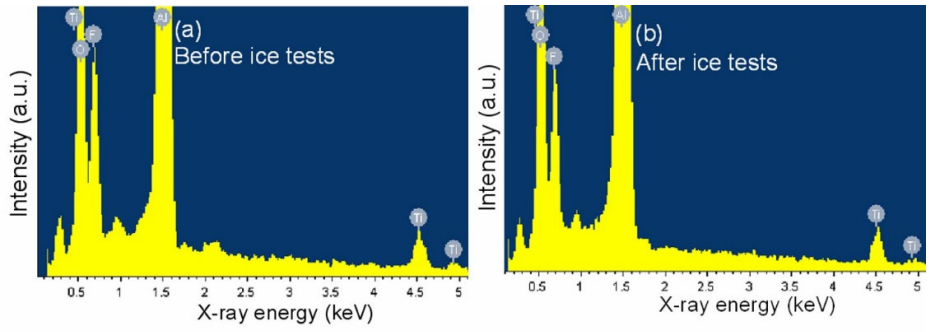

Figure 8. EDX spectra of Tef/TiO_2/ns-Al (**a**) before and (**b**) after ice adhesion tests.

4. Conclusions

AA6061 aluminum alloy surfaces (with or without a TiO_2 coating) were rendered superhydrophobic by creating a certain rough nanostructure on the aluminum alloy surface by chemical etching and by lowering the surface energy by applying a coating of rf-sputtered Teflon® to reduce the affinity of water, preventing water (and ice) sticking to

these surfaces. The nanostructured feature on the textured surfaces was confirmed from FESEM images, and the presence of TiO_2 and rf-sputtered Teflon® was confirmed by XPS analyses. Contact angles >160° and contact angle hystereses <5° were obtained on these surfaces with water roll-off properties. The icephobicity tests conducted on these surfaces showed no formation of ice on superhydrophobic surfaces, indicating zero adhesion while ice formed and accumulated on hydrophilic counterparts with very high ice adhesion strengths of >400 kPa comparable to that obtained on bare aluminum. The results and observations of this study show that superhydrophobic surfaces governed by geometry (textured) and chemistry (low surface energy) are promising candidates for icephobic applications. The possibility of applying an intermediate oxide layer (TiO_2 in this study) shows potentials for application on insulating surfaces in addition to metallic surfaces.

Author Contributions: Data acquisition, N.S., D.K.S.; Investigation, N.S., D.K.S. All authors have read and agreed to the published version of the manuscript.

Funding: This research was funded by Natural Sciences and Engineering Research Council of Canada (NSERC), Hydro-Québec, and all the partners of the Industrial Chair on Atmospheric Icing of Power Network Equipment (CI-GELE) and Canada Research Chair on Engineering of Power Network Atmospheric Icing (IN-GIVRE).

Institutional Review Board Statement: Not applicable.

Informed Consent Statement: Not applicable.

Data Availability Statement: Reference #1: Saleema, N. Nanostructured Thin Films for Icephobic Applications. Ph.D. thesis, University of Quebec, Quebec, Canada, January 2009.

Acknowledgments: The authors thank the Natural Sciences and Engineering Research Council of Canada (NSERC), Hydro-Québec, and all the partners of the Industrial Chair on Atmospheric Icing of Power Network Equipment (CIGELE) and Canada Research Chair on Engineering of Power Network Atmospheric Icing (INGIVRE) for their financial support. We also thank M. Farzaneh (CIGELE, UQAC) for providing the materials preparation and ice testing facilities, R.W. Paynter of INRS Varennes (QC) for XPS facilities; and K.G.M. Nair of Indira Gandhi Center for Atomic Research (IGCAR), India, for the RBS and XRD measurements.

Conflicts of Interest: The authors declare no conflict of interest.

References

1. Saleema, N. Nanostructured Thin Films for Icephobic Applications. Ph.D. thesis, University of Quebec, Chicoutimi, Quebec, Canada, January 2009.
2. Petrenko, V.F.; Qi, S. Reduction of ice adhesion to stainless steel by ice electrolysis. *J. Appl. Phys.* **1999**, *86*, 5450, doi:10.1063/1.371544.
3. Yoshida, S.; Naito, K. Survey of electrical and mechanical failures of insulators caused by ice and/or snow. *CIGRE WG B*, **2005**, 2, 22–26.
4. Farzaneh, M.; Melo, O.T. Flashover performance of insulators in the presence of short icicles. *Int. J. Offshore Polar Eng.* **1993**, *4*, No. ISOPE-94-04-2-112.
5. Mendes, P.M.; Yeung, C.L.; Preece, J.A. Bio-nanopatterning of surfaces. Nanoscale Res. Lett. **2007**, *2*, 373, doi:10.1007/s11671-007-9083-3.
6. Volat, C.; Farzaneh, M.; Leblond, A. De-icing/anti-icing techniques for power lines: Current methods and future direction. In Proceedings of the 10th International Workshop on Atmospheric Icing of Structures (IWAIS XI), Montréal, Québec, Canada, June 2005, https://www.compusult.com/html/IWAIS_Proceedings/IWAIS_2005/Papers/IW20.PDF.
7. Saleema, N.; Farzaneh, M.; Paynter, R.W.; Sarkar, D.K. Prevention of ice accretion on aluminum surfaces by enhancing their hydrophobic properties. *J. Adhes. Sci. Technol*. **2011**, *25*, 27–40.
8. Sarkar, D.K.; Saleema, N.M. A review on the fabrication of nanostructured superhydrophobic aluminum surfaces. In *Recent Advances in Adhesion Science and Technology in Honor of Dr. Kash Mittal*; Gutowski, W.V., Dodiuk, H., Eds.; CRC Press: FL, USA, 2014, pp. 83–124, (Print ISBN: 978-90-04-20173-6.
9. Saleema, N.; and Farzaneh, M. Thermal effect on superhydrophobic performance of stearic acid modified ZnO nanotowers. *Appl. Surf. Sci*. **2008**, *254*, 2690–2695.
10. Sarkar, D.K.; Farzaneh M. Superhydrophobic coatings with reduced ice adhesion. *J. Adhes. Sci. and Technol.* **2009**, *23*, 1215–1237.
11. Zhuo, Y.Z.; Xiao, S.B.; Amirfazli, A.; He, J.Y.; Zhang, Z.L. Polysiloxane as icephobic materials–The past, present and the future. Chem. Eng. J. **2021**, *405*, 127088.

12. Cao P.; Chen Z.; Cao H.; Chen B.; Zheng Z. Anti-icing performance of hydrophobic material used for electromechanical drill applied in ice core drilling. J. of Glaciol. **2020**, *66*, 618–626.
13. Barthlott, W.; Neinhuis, C. Purity of the sacred lotus, or escape from contamination in biological surfaces. Planta **1997**, *202*, 1–8.
14. Zheng, Y.; Gao, X.; Jiang, L. Directional adhesion of superhydrophobic butterfly wings. Soft Matter **2007**, *3*, 178–182.
15. Sarkar, D.K.; Farzaneh, M.; Paynter, R.W. Superhydrophobic properties of ultrathin rf-sputtered Teflon films coated etched aluminum surfaces. Mater. Lett. **2008**, *62*, 1226–1229.
16. Wang, Y.; Liu, X.W.; Zhang, H.F.; Zhou, Z.P. Fabrication of super-hydrophobic surfaces on aluminum alloy substrates by RF sputtered polytetrafluoroethylene coatings. AIP Adv. **2014**, *4*, 031323.
17. Ratova, M.; Kelly, P.J.; West, G.T. Superhydrophobic photocatalytic PTFE–titania coatings deposited by reactive pDC magnetron sputtering from a blended powder target. Mater. Chem. and Phys. **2017**, *190*, 108–113.
18. Petrenko, V.F.; Whitworth, R.W. Physics of Ice. Oxford University press: New York, NY, USA, 1999, ISBN: 0-19-851895-1.
19. *User Manual for Drop Shape Analyzer*. V1.9-03; KRUSS GmbH: Hamburg, Germany, 2004.
20. Laforte, C.; Beisswenger, A. Icephobic material centrifuge adhesion test. In Proceedings of the International Workshop on Atmospheric Icing of Structures (IWAIS XI), Montréal, Québec, Canada, June 2005**,** https://www.compusult.com/html/IWAIS Proceedings/IWAIS_2005/Papers/IW53.PDF.
21. Saleema, N.; Sarkar, D.K.; Gallant, D.; Paynter, R.W.; Chen, X.G. Chemical nature of superhydrophobic aluminum alloys surfaces produced via a one-step process using fluoroalkyl-silane in a base medium. *ACS Appl. Mater. Interfaces* **2011**, *3*, 4775–4781.
22. Sarkar, D.K.; Brassard, D.; El-Khakani, M.A.; Ouellet, L. Dielectric properties of sol–gel derived high-k titanium silicate thin films. *Thin Solid Films* **2007**, *515*, 4788–4793.
23. El-Khakani, M.A.; Sarkar, D.K.; Ouellet, L.; Brassard, D. Titanium silicate films with high dielectric constant. US Patent 7,101,754 5 September 2006.
24. Wang, X.; Zuo, J.; Keil, P.; Grundmeier, G. Comparing the growth of PVD silver nanoparticles on ultra-thin fluorocarbon plasma polymer films and self-assembled fluoroalkyl silane monolayers. *Nanotechnol*. **2007**, *18*, 265303.
25. Cassie A.B.D.; Baxter, S. Wettability of porous surfaces. *Trans. Faraday Soc*. **1944**, *40*, 546–551.
26. Petrenko, V.; Peng, S. Reduction of ice adhesion to metal by using self-assembling monolayers (SAMs). *Can. J. Phys*. **2003**, *81*, 387–393.
27. Somlo, B.; Gupta, V. A hydrophobic self-assembled monolayer with improved adhesion to aluminum for deicing application. *Mech. Mater*. **2001**, *33*, 471–480.
28. Javan-Mashmool, M.; Volat, C.; Farzaneh, M. A new method for measuring ice adhesion strength at an ice-substrate interface. *Hydrol. Process*. **2006**, *20*, 645–655.
29. Itagaki, K. The implications of surface energy in ice adhesion. *J. Adhes*. **1983**, *16*, 41–48.
30. Bain, C.D.; Whitesides, G.M. Depth sensitivity of wetting: monolayers of omega-mercapto ethers on gold. *J. Am. Chem. Soc*. **1988**, *110*, 5897–5898.
31. Jafari, R.; Farzaneh, M. Fabrication of superhydrophobic nanostructured surface on aluminum alloy. *Appl. Phys*. A **2011**, *102*, 195–199.
32. Milles, S.; Marcos S.; Voisiat B.; Lasagni, A.F. Fabrication of superhydrophobic and ice-repellent surfaces on pure aluminium using single and multiscaled periodic textures. *Sci. Rep*. **2019**, *9*, 1–13.